



**HAL**  
open science

## Plasmacytoid Dendritic Cell Infection and Sensing Capacity during Pathogenic and Nonpathogenic Simian Immunodeficiency Virus Infection.

Simon P Jochems, Beatrice Jacquelin, Lise Chauveau, Nicolas Huot, Gaël Petitjean, Alice Lepelley, Anne-Sophie Liovat, Mickaël J Ploquin, Emily K Cartwright, Steven E Bosinger, et al.

► **To cite this version:**

Simon P Jochems, Beatrice Jacquelin, Lise Chauveau, Nicolas Huot, Gaël Petitjean, et al.. Plasmacytoid Dendritic Cell Infection and Sensing Capacity during Pathogenic and Nonpathogenic Simian Immunodeficiency Virus Infection.. *Journal of Virology*, 2015, 89 (13), pp.6918-27. 10.1128/JVI.00332-15 . pasteur-01219427

**HAL Id: pasteur-01219427**

**<https://pasteur.hal.science/pasteur-01219427>**

Submitted on 22 Oct 2015

**HAL** is a multi-disciplinary open access archive for the deposit and dissemination of scientific research documents, whether they are published or not. The documents may come from teaching and research institutions in France or abroad, or from public or private research centers.

L'archive ouverte pluridisciplinaire **HAL**, est destinée au dépôt et à la diffusion de documents scientifiques de niveau recherche, publiés ou non, émanant des établissements d'enseignement et de recherche français ou étrangers, des laboratoires publics ou privés.

Copyright

1 **Plasmacytoid dendritic cell infection and sensing capacity during pathogenic and non-**  
2 **pathogenic SIV infection**

3 **Running title: Low AGM pDC CD4 and CCR5 levels allow SIV infection**

4 Simon P. Jochems<sup>1,2</sup>, Beatrice Jacquelin<sup>1</sup>, Lise Chauveau<sup>3</sup>, Nicolas Huot<sup>4</sup>, Gaël Petitjean<sup>5,§</sup>, Alice  
5 Lepelley<sup>3,§</sup>, Anne-Sophie Liovat<sup>5</sup>, Mickaël J. Ploquin<sup>1</sup>, Emily K. Cartwright<sup>6</sup>, Steven E. Bosinger<sup>6,7</sup>,  
6 Guido Silvestri<sup>6</sup>, Françoise Barré-Sinoussi<sup>5</sup>, Pierre Lebon<sup>8</sup>, Olivier Schwartz<sup>3</sup> and Michaela C.  
7 Müller-Trutwin<sup>1,#</sup>

8 <sup>1</sup>Institut Pasteur, Unité HIPER, Paris, France <sup>2</sup>Université Paris Diderot, Sorbonne Paris Cité. <sup>3</sup>  
9 Institut Pasteur, Unité VI, Paris, France. <sup>4</sup>IDMIT, CEA, France. <sup>5</sup>Institut Pasteur, Unité RIR, Paris,  
10 France. <sup>6</sup>Division of Microbiology and Immunology, Emory Vaccine Center, Yerkes NPRC. <sup>7</sup>Non-  
11 Human Primate Genomics Core, Yerkes NPRC, Atlanta, Georgia, USA. <sup>8</sup>Laboratoire de Virologie,  
12 Hôpital Saint-Vincent de Paul and Université Paris Descartes, Paris, France.

13 #, Corresponding author: Michaela Müller-Trutwin, michaela.muller-trutwin@pasteur.fr

14 §Current affiliations and addresses for authors whose affiliations have changed since  
15 completion of the study: Gaël Petitjean, Laboratory of Molecular Virology, Institute of human  
16 genetics, CNRS UPR 1142, Montpellier, France. Alice Lepelley, Department of Microbiology and  
17 Immunology, Columbia University, NY, USA

18 Word count abstract = 199

19 Word count importance = 146

20 Word count text = 3590

21 **Abstract**

22 HIV in humans and SIV in macaques (MAC) lead to chronic inflammation and AIDS. Natural  
23 hosts, such as African green monkeys (AGM) and sooty mangabeys (SM), are protected against  
24 SIV-induced chronic inflammation and AIDS. Here, we report that AGM plasmacytoid dendritic  
25 cells (pDC) express extremely low levels of CD4, unlike MAC and human pDC. Despite this, AGM  
26 pDC efficiently sensed SIVagm, but not heterologous HIV/SIV isolates, indicating a virus-host  
27 adaptation. Moreover, both AGM and SM pDC were found to be, in contrast to MAC pDC,  
28 predominantly negative for CCR5. Despite such limited CD4 and CCR5 expression, lymphoid  
29 tissue pDC were infected to a similar degree as CD4<sup>+</sup> T cells, both in MAC and AGM. Altogether,  
30 our finding of efficient pDC infection by SIV *in vivo* identifies pDC as a potential viral reservoir in  
31 lymphoid tissues. We discovered low expression of CD4 on AGM pDC, which did not preclude  
32 efficient sensing of host-adapted viruses. Therefore, pDC infection and efficient sensing are not  
33 prerequisites for chronic inflammation. The high level of pDC infection by SIVagm suggests that  
34 if CCR5 paucity on immune cells is important for non-pathogenesis of natural hosts, it is possibly  
35 not due to its role as a co-receptor.

36 **Importance**

37 The ability of certain key immune cell subsets to resist infection might contribute to the  
38 asymptomatic nature of simian immunodeficiency virus (SIV) infection in its natural hosts, such  
39 as African green monkeys (AGM) and sooty mangabeys (SM). This relative resistance to  
40 infection has been correlated with reduced expression of CD4 and/or CCR5. We show that  
41 plasmacytoid dendritic cells (pDC) of natural hosts display a reduced CD4 and/or CCR5  
42 expression, unlike macaque pDC. Surprisingly, this did not protect AGM pDC, as infection levels

43 were similar to those found in MAC pDC. Furthermore, we show that AGM pDC did not  
44 consistently produce IFN-I upon heterologous SIVmac/HIV-1 encounter, while they sensed  
45 autologous SIVagm isolates. Pseudotyping SIVmac/HIV-1 overcame this deficiency, suggesting  
46 that reduced uptake of heterologous viral strains underlay this lack of sensing. The distinct IFN-I  
47 responses depending on host species and HIV/SIV isolates reveal host/virus species-specificity of  
48 pDC sensing.

## 49 **Introduction**

50 Chronic inflammation and immune activation in HIV-infected individuals and in SIV-infected  
51 macaques (MAC) lead to depletion of CD4<sup>+</sup> T cells and progression to AIDS. Natural hosts of SIV,  
52 such as African green monkeys (AGM) and sooty mangabeys (SM), do not display chronic  
53 inflammation or AIDS (1). This is due to resolution of inflammation before the end of acute  
54 infection, rather than to a lack of SIV recognition by the innate immune system (2). Natural  
55 hosts further differ from pathogenic HIV/SIV infections by exhibiting reduced infection rates in  
56 certain cell subsets, such as central memory CD4<sup>+</sup> T cells (T<sub>cm</sub>) (3, 4). This relative resistance has  
57 been linked to a reduced expression of the HIV/SIV co-receptor CCR5 on natural host CD4<sup>+</sup> T  
58 cells and to a downmodulation of CD4 on activated CD4<sup>+</sup> T cells in AGM (3-5).

59 Plasmacytoid dendritic cells (pDC) form a rare cell population that is responsible for the vast  
60 majority of IFN-I production after HIV encounter (6). This is also true for AGM pDC as the  
61 depletion of pDC from AGM PBMC completely abrogates the IFN-I response to SIVagm  
62 stimulation (7). HIV/SIV sensing by pDC is mediated through endocytosis followed by TLR7/9  
63 engagement. It requires CD4, but is independent of co-receptor expression (6). Data on the  
64 infection rates of pDC *in vivo* are scarce. One study reported the presence of HIV DNA in

65 circulating pDC of chronically HIV-infected patients (8). Another study reported high infection  
66 levels in lymph node (LN) pDC during acute SIVmac infection (9).

67 Here, we discovered a restricted CD4 and/or CCR5 expression on pDC in natural hosts. We  
68 evaluated the effect of low CD4 expression on the capacity of AGM pDC to efficiently sense  
69 distinct forms of SIVagm (free virus, non-infectious particles and SIVagm-infected cells).  
70 Furthermore, we examined the infection frequency of pDC during pathogenic and non-  
71 pathogenic SIV infection.

## 72 **Materials and Methods**

### 73 **Study Approval**

74 All animal experimental protocols were approved by either the Ethical Committee of Animal  
75 Experimentation (CETEA-DSV, IDF, France) (Notification numbers: 10-051b and 12-006) or by the  
76 Institutional Animal Care and Use Committees (IACUC) of Emory University (IACUC protocol  
77 #2000793, entitled “Comparative AIDS Program”). Animals were housed in the facilities of the  
78 CEA (“Commissariat à l’Energie Atomique”, Fontenay-aux-Roses, France, permit number: A 92-  
79 032-02), Institut Pasteur (Paris, France, permit number: A 78-100-3) or Yerkes National Primate  
80 Research Center (Atlanta, GA, USA). All experimental procedures were conducted in strict  
81 accordance with the international European guidelines 2010/63/UE on protection of animals  
82 used for experimentation and other scientific purposes (French decree 2013-118) and with the  
83 recommendations of the Weatherall report or in strict accordance with USDA regulations and  
84 the recommendations in the Guide for the Care and Use of Laboratory Animals of the National  
85 Institutes of Health. The CEA complies with Standards for Human Care and Use of Laboratory of

86 the Office for Laboratory Animal Welfare (OLAW, USA) under OLAW Assurance number #A5826-  
87 01. The monitoring of the animals was under the supervision of the veterinarians in charge of  
88 the animal facilities.

#### 89 **In vivo infections and sample collection**

90 Twenty-six African green monkeys (*Chlorocebus sabaeus*) of the sabaeus species with a  
91 Caribbean origin, eighttteen Chinese rhesus macaques (*Macaca mulatta*), two cynomolgous  
92 macaques (*Macaca fascularis*), sixteen Indian rhesus macaques (*Macaca mulatta*) and sixteen  
93 sooty mangabeys (*Cercocebus atys*) were used in this study. Eleven AGMs were infected via  
94 intravenous inoculation with 250 TCID<sub>50</sub> of SIVagm.sab92018, as described previously (10, 11).  
95 Four Chinese rhesus macaques were i.v. infected with 50 AID<sub>50</sub> SIVmac251 and two others were  
96 infected with 5000 AID<sub>50</sub> SIVmac251, as described previously (10, 12). Eight Indian rhesus  
97 macaques had been previously infected with SIVmac239 or SIVmac251 and eight sooty  
98 mangabeys were either naturally infected or infected experimentally with SIVsmE041 (13, 14).  
99 Blood was collected by venipuncture on sodium heparin tubes and shipped to Institut Pasteur or  
100 used on site at Yerkes National Primate Research Center. Bone marrow mononuclear cells were  
101 isolated on Ficoll and tissue cells were put in suspension before staining. LNs and spleens were  
102 disrupted mechanically and rectal tissues were enzymatically degraded as described previously  
103 (12, 15).

#### 104 **Viral stimulations**

105 Freshly isolated PBMCs were cultured at 0.5x10<sup>6</sup> cells/well in 24-well plates (Costar) at 37° C, 5%  
106 CO<sub>2</sub> for eighteen hours with or without virus. Cell viability was measured using trypan blue and a  
107 Countess (Life Technologies) cell counter. The SIVagm strains used, have been previously

108 described: SIVagm.sab92018 (11), SIVagm.sabD46 and SIVagm.tanB14 (16), SIVagm.sab1c (11,  
109 17) and SIVgri1 (18, 19). Free SIVagm was added to PBMCs at a concentration of 1500 ng/mL  
110 p27, unless indicated otherwise. HSV-1 was added at a TCID<sub>50</sub> of 2x10<sup>5</sup>. HIV-1.Bal-VSV, which is  
111 endocytosed independently of CD4 (20), was kindly provided by A. David and AT2-inactivated  
112 SIVagm as well as control microvesicles by Dr. Jeff Lifson (National Cancer Institute, Frederick,  
113 MD). SIVmac251-VSV was produced by co-transfecting 293T cells with SIVmac251Δenv and VSV-  
114 G expression vector using SuperFect (Qiagen), as described previously (21). SIVagm isolates  
115 were grown on SupT1 cells, as these cells express Bonzo and are susceptible to SIVagm while  
116 SIVmac isolates were grown on CEMx174 as these cells express Bob and are susceptible to  
117 SIVmac (22).

#### 118 **Production of infected cells**

119 Cells were infected as previously described (23). Briefly, SupT1 cells were exposed for one hour  
120 at 37° C to 3.3x10<sup>4</sup> TCID<sub>50</sub> per 10<sup>6</sup> cells under constant agitation. Infection levels were assessed  
121 by measuring SIV Gag<sup>+</sup> cells using flow cytometry (see below).

#### 122 **Functional Interferon alpha assay**

123 Bioactive IFN-I levels were quantified as described earlier (7). In short, Mardin-Darby Bovine  
124 Kidney (MDBK) cells were incubated with UV-inactivated supernatants for 18 hours, after which  
125 the cytopathic effect of vesicular stomatic virus was determined using the CellTiter 96®  
126 AQueous Non-Radioactive Cell Proliferation Assay (Promega). Alternatively, a cell line stably  
127 transfected with a luciferase gene under an IFN-I inducible promoter was used to measure IFN-I  
128 levels, as described previously (23). The limit of detection threshold was set at 2 IU/mL.

#### 129 **Flow cytometry**

130 SM flow cytometric data were acquired at Yerkes National Primate Center and data for AGM  
131 were acquired at Institut Pasteur. MAC data were acquired at both Yerkes and Pasteur, with  
132 similar results. The following antibodies were used to identify and characterize pDC phenotype  
133 and function in whole blood or isolated tissue cells: CD3 (SP34-2), CD4 (L200), HLA-DR (L243),  
134 CCR5 (3A9), CD123 (7G3) (all BD Biosciences), CD20 (2H7, ebioscience), CD4 (M-T466), BDCA-2  
135 (AC144) (all Miltenyi) and CD4 (SFC112T4D11, Beckman Coulter). FcR Blocking Reagent (Miltenyi)  
136 was used to block unspecific antibody binding and in experiments using tissues other than  
137 blood, Live/Dead cell viability (Invitrogen) was used to exclude dead cells. For intracellular  
138 staining, cells were labeled with surface-binding antibodies and fixed with 4%  
139 paraformaldehyde and permeabilized using saponin prior to incubation with anti-CD4. For  
140 intracellular SIVagm detection, anti-p24 staining (KC57, Beckman Coulter) was used after cell  
141 permeabilization with the IntraPrep Permeabilization Reagent Kit (Beckman Coulter) according  
142 to manufacturer's instructions (23). Events ranging from one hundred to one thousand pDC  
143 were collected on a BD LSR-II flow cytometer, running BD FACS Diva 6.0 software, and analyzed  
144 with FlowJo 9.4.10 (TreeStar). Anti-mouse compensation beads (BD Biosciences) and Arc Amine  
145 Reactive Compensation Bead Kit (Life Technologies) were used to define compensation levels.  
146 An isotype control antibody was used to define CCR5<sup>+</sup> cells.

#### 147 **Cell sorting**

148 Splenocytes were frozen in 10% DMSO in liquid nitrogen until use. Cells were thawed in the  
149 presence of DNase I (10 IU/mL, Roche) and washed in FCS. Cells were labeled with antibodies  
150 against CD3, CD20, HLA-DR, CD4, CD123 and with Live/Dead reagent in the presence of FcR  
151 Blocking Reagent. Cells were sorted using a FACSAria II sorter (BD), running on BD FACS Diva 6.0



152 software. Sorted pDC and CD4<sup>+</sup> T cells were purified a second time to increase purity of the two  
153 fractions. CD4<sup>+</sup> T cells were also isolated from LNs cells using anti-CD4 beads and magnetic  
154 stands (Miltenyi) following manufacturer's protocol, after which purity was verified by flow  
155 cytometry.

#### 156 **SIV DNA quantification**

157 DNA was extracted as follows: samples were lysed in NaCl (3M), EDTA (0.5M, pH 8), SDS (10%,  
158 Bio-Rad) and proteinase K (1mg/mL, Qiagen) in a 45 min incubation at 55 ° C. Then, NaCl (5M)  
159 was added and incubated at 4 ° C between 15 and 60 min, followed by centrifugation for 15  
160 min at 3000 rpm at 4 ° C. DNA was then precipitated from the supernatant in  
161 phenol:chloroform:isoamyl alcohol 25:24:1 (pH = 8, Sigma Aldrich). After DNA extraction, viral  
162 DNA was measured by qPCR in duplicate, using primers and probes designed specifically for  
163 SIVagm.sab and SIVmac (11, 15). SIVagm and SIVmac plasmids were used as standards to  
164 calculate SIV DNA copy numbers. CCR5 DNA quantification was used to normalize the viral levels  
165 to the number of cells (24). Sample preparation, enzyme mix preparation and PCR set-up were  
166 performed in three separate rooms to avoid PCR contamination. Positive and negative controls  
167 were used to exclude sample contamination.

#### 168 **Fluorescence microscopy**

169 Fluorescence microscopy was done as follows with markers against NKp30 (AF29-4D12,  
170 Miltenyi), CD123 (5B11, Biolegend), DAPI and SIVagm *env* RNA (made from the region amplified  
171 by 5'-GAG GCT TGT GAT AAA ACT TAT TGG GAT-3' and 5'-AGA GCA GTG ACG CGG GCA TTG  
172 AGG-3' primers and labeled with fluorochrome Alexa 488 (Life Technologies)). Briefly,  
173 cryopreserved sections were permeabilized by incubating in 0.5% (v/v) Triton X-100. This was

174 followed by hybridization of probe and mounted antibodies on tissue. Secondary antibodies  
175 were used with to visualize the bound antibodies. Donkey anti-mouse IgG-CFL 594 (Santa Cruz)  
176 was used to detect CD123 and Zenon Alexa Fluor 647 Mouse IgG1 Labeling Kit (Life  
177 technologies) to reveal the NKP30 antibody. As negative controls for SIV RNA in situ  
178 hybridization, we used a RNase degraded probe, taken up in hybridization buffer, as well as  
179 lymph nodes of uninfected animals. Images were acquired on a Confocal Laser Scanning  
180 Microscope Leica TCS SP8, running LAS AF 3 (Leica Application Suite Advanced Fluorescence).

## 181 **Statistics**

182 Statistical inference analyses were performed using Prism 5.0 (GraphPad). The non-parametric  
183 Wilcoxon signed rank test and Mann-Whitney test were used to test paired and non-paired  
184 observations, respectively. In case of multiple testing of unpaired data, a non-parametric  
185 Kruskal-Wallis test, followed by a Dunn's multiple comparison test, was used. Multiple testing of  
186 paired data without missing values was done by a Friedman test, followed by a Dunn's multiple  
187 comparison test.

## 188 **Results**

### 189 **Low CD4 expression on AGM pDC**

190 Given the importance of CD4 for HIV/SIV sensing by pDC, we measured CD4 on pDC from  
191 uninfected AGM, SM and MAC (Figure 1). PDC were defined as CD3<sup>-</sup>CD20<sup>-</sup>HLA-DR<sup>+</sup>CD123<sup>hi</sup> cells  
192 (Figure 2A) (2). MAC and SM pDC displayed similar CD4 levels as on CD4<sup>+</sup> T cells (Figure 1A and  
193 B). Surprisingly, AGM pDC expressed CD4 at >1 log lower levels than CD4<sup>+</sup> T cells ( $p < 0.001$ ).

194 As (i) CD4 MFI on CD4<sup>+</sup> T cells was similar between AGM and MAC and (ii) two additional CD4  
195 antibody clones confirmed low CD4 expression on AGM pDC (Figure 2B), it is unlikely that low  
196 CD4 on AGM pDC was due to species-specific antibody issues. The absence of intracellular CD4  
197 in AGM pDC indicated that recycling from the cell surface was not the underlying mechanism of  
198 this low expression (Figure 2C). AGM pDC from primary, secondary and tertiary lymphoid tissues  
199 all expressed low levels of CD4 (Figure 2D).

#### 200 **Efficient SIV-sensing by AGM pDC**

201 The low CD4 expression on AGM pDC is paradoxical, since CD4 is essential for HIV/SIV sensing by  
202 pDC and AGM pDC have been shown to efficiently sense SIVagm (7, 12). Nonetheless, a lower  
203 production of IFN-I has been described during SIVagm infection *in vivo* (12, 25). We wondered  
204 whether low CD4 on pDC could have subtle effects on SIV sensing *in vivo*. For instance, only  
205 sensing of infectious SIVagm particles has been investigated (12, 25), while (i) most virions  
206 produced *in vivo* are non-infectious and (ii) sensing of virus-infected cells is more efficient in  
207 human and MAC (23). We stimulated peripheral blood mononuclear cells (PBMC) of a large  
208 number of uninfected AGM and MAC with infectious SIV, using HSV as a control for CD4-  
209 independent sensing. No quantitative differences in IFN-I production were observed between  
210 AGM and MAC (Figure 3A). Both SIV-infected cells and AT2-inactivated SIVagm also induced  
211 normal IFN-I responses (Figures 3B and 3C). Longitudinal measurement showed that CD4 levels  
212 on pDC did not further decrease during SIV infection (Figure 3D). Altogether, these data  
213 demonstrate that low CD4 on AGM pDC did not impair their capacity to sense SIVagm.

#### 214 **SIV isolate-dependent sensing of AGM pDC**

215 We wondered how SIVagm is sensed by pDC despite low CD4 expression. CD4 is a highly  
216 polymorphic molecule among primates. We raised the hypothesis that given the long circulation  
217 of SIVagm in the AGM population, SIVagm is well-adapted to AGM CD4 (26). This could entail  
218 that SIVagm, but not heterologous viruses, can elicit robust IFN-I responses by AGM pDC. We  
219 tested this hypothesis by stimulating AGM (sabraeus) and MAC PBMC with nine SIV/HIV isolates  
220 (Figure 4A, B). The three SIVagm.sab isolates and the SIVagm.tan isolate induced robust IFN-I  
221 production by AGM pDC. SIVagm.gri did not induce an efficient response, which corresponds  
222 with the observation that the *CD4* genes of the sabraeus and tantalus AGM species are more  
223 closely related to each other than to the *CD4* gene of the grivet AGM species (26).

224 In contrast, HIV-1 and two out of three SIVmac (SIVmac.251 and SIVmac.STM) isolates did not  
225 induce robust IFN-I production by AGM pDC ( $p < 0.05$  or  $p < 0.01$ ), even at a high viral dose. Only  
226 SIVmac239 induced IFN-I production from AGM PBMC, already at a low viral dose. Low dose of  
227 SIVmac239 also induced high levels of IFN-I in by MAC PBMC. At the highest dose, SIVmac239  
228 was more cytotoxic for AGM PBMC than SIVmac251 ( $p < 0.05$ , Figure 4C). However, at a dose of  
229 150 ng/mL p27, SIVmac239 did not influence viability, so it is unlikely that the strong response  
230 to SIVmac239 was related to dying cells, which are known to induce IFN-I responses (Figure 4C).  
231 It should be noted that SIVmac239 has been shown to be highly virulent *in vivo* compared to  
232 SIVmac251 (27). In contrast to AGM pDC, MAC pDC produced IFN-I upon stimulation with all  
233 SIV/HIV isolates, including SIVagm (Figure 4B).

234 If the lack of SIVmac/HIV sensing by AGM pDC is indeed due to low CD4, then forcing viral  
235 endocytosis should overcome this sensing deficiency. In line with this, HIV-1, or SIVmac251,  
236 pseudotyped with VSV-G were sensed similar to SIVagm (Figure 4D). Indeed, pseudotyped HIV-1

237 and SIVmac251 induced higher levels of IFN-I than their wild-type isolates ( $p < 0.05$  and  $p < 0.01$ ,  
238 respectively, Figure 4D). Altogether, these findings indicate a virus-host co-adaptation in AGM  
239 for viral sensing by pDC.

#### 240 **Predominance of CCR5 negative pDC in natural hosts**

241 We next examined CCR5 expression on AGM pDC, since co-receptor expression, in addition to  
242 CD4, is essential for infection. MAC pDC were predominantly CCR5<sup>+</sup> (median 92.3%), while the  
243 majority of AGM and SM pDC did not express detectable levels of CCR5 (7.7% and 40% CCR5<sup>+</sup>  
244 pDC, respectively; Figure 1A and 1C). In SMs, the percentage of CCR5<sup>+</sup> pDC was lower after SIV  
245 infection (18.4%,  $p = 0.02$ ; Figure 1C).

#### 246 **pDC are highly infected during pathogenic and non-pathogenic SIV infection**

247 We then addressed the question if these reduced CD4 and CCR5 expressions associate with low  
248 infection of AGM pDC. To test this, we purified splenic pDC and CD4<sup>+</sup> T cells of chronically SIV-  
249 infected AGM and MAC and measured cell-associated viral DNA. Cells from uninfected animals  
250 were never positive for viral DNA (data not shown). Spleen pDC and CD4<sup>+</sup> T cells from MAC  
251 harbored a median of  $8.1 \times 10^4$  and  $9.2 \times 10^3$  copies per million cells, respectively ( $p = 0.37$ ,  
252 Figure 5A). AGM harbored  $3.2 \times 10^4$  and  $4.1 \times 10^3$  copies per million splenic pDC and CD4<sup>+</sup> T  
253 cells, respectively ( $p = 0.44$ , Figure 5A). AGM and MAC pDC were thus infected to a similar  
254 extent *in vivo*. As infection levels were similar between pDC and CD4<sup>+</sup> T cells, potentially  
255 contaminating CD4<sup>+</sup> T cells in the pDC fraction cannot explain the levels of detected SIV DNA in  
256 pDC. As pDC have limited phagocytic capacities, the high levels of viral DNA in these cells are  
257 also unlikely to be associated with engulfed infected T cells.

258 To further demonstrate the infection status of AGM pDC, we immunohistochemically examined  
259 a LN of a chronically infected AGM (Figure 5B). CD123 and SIVagm RNA signals overlapped,  
260 while NKp30, which is not expressed on pDC, did not co-stain with CD123 or SIVagm RNA.

261 We then measured CD4 and CCR5 expression on splenic pDC of chronically infected AGM and  
262 MAC to exclude phenotypic differences compared to pDC from blood or from lymphoid tissues  
263 of uninfected animals. Splenic pDC of SIV-infected AGM, but not MAC, expressed low levels of  
264 CD4 (Figure 6). Only 4.7% of AGM splenic pDC had detectable CCR5 expression, while 92.9% of  
265 MAC splenic pDC were CCR5<sup>+</sup> ( $p = 0.0079$ ). In conclusion, pDC of AGM and MAC were infected  
266 at high levels despite a restricted CD4 and CCR5 expression on AGM pDC.

## 267 **Discussion**

268 Such low CD4 expression as the one we discovered on AGM pDC is remarkable given the  
269 evolutionary conserved high expression of CD4 on mammalian pDC, including primate, murine,  
270 cattle and swine pDC (6, 28, 29). The role of CD4 in pDC biology is currently unknown, but this  
271 low expression raises questions on the physiological impact for AGM. The low CD4 levels on pDC  
272 were sufficient to allow SIVagm endocytosis and subsequent sensing and we demonstrated for  
273 the first time that natural host pDC can sense SIV-infected cells. In contrast, most SIVmac and  
274 HIV-1 isolates tested were not sensed by AGM pDC. Pseudotyping increased the efficiency of  
275 HIV-1/SIVmac251 sensing, which indicates that inefficient sensing of heterologous virus was due  
276 to restricted viral uptake. Altogether, this suggests an adaptation between SIVagm and its host-  
277 specific CD4. Similar to our findings, it has been shown that HIV-1 poorly interacts with MAC  
278 CD4 compared to human CD4 and that HIV-1 could thus infect cells expressing low levels of  
279 human CD4, but not cells expressing low levels of MAC CD4 (30). Low CD4 expression also did

280 not prevent AGM pDC from being infected as they were infected at high levels *in vivo*. Since the  
281 pDC sensing capacity and infection levels were similar between AGM and MAC, these factors do  
282 not determine the level of chronic inflammation.

283 Our study reveals a high infection rate of pDC in secondary lymphoid tissue during chronic SIV  
284 infection. These data resemble those of acute SIVmac infection, where pDC were found to be  
285 infected to similar levels as CD4<sup>+</sup> T cells in LN (9). Since only very few data on pDC infection *in*  
286 *vivo* are available, this is important and underlines the potential role of pDC as a viral reservoir.  
287 Of note, the ratio of pDC to CD4<sup>+</sup> T cells is low, approximately 1:300 in lymph nodes (2).  
288 Therefore, the majority of viral burden in SIV infection is still associated with CD4<sup>+</sup> T cells.  
289 However the contribution of pDC should not be underestimated, given their presence in  
290 mucosae, their capacity to migrate to lymph nodes and their ability to efficiently transmit  
291 HIV/SIV to CD4<sup>+</sup> T cells.

292 The lack of correlation between the frequency of CCR5<sup>+</sup> pDC and SIV infection status does not  
293 support the hypothesis that absence of CCR5 expression protects against target cell infection  
294 (4). In line with this, a mutation in the SM CCR5 allele, disrupting functional CCR5 expression,  
295 does not diminish SIVsm infection prevalence (31). This can be explained by the fact that SIVs,  
296 including SIVagm, efficiently use alternative co-receptors, such as CXCR6 (Bonzo) and GPR15  
297 (BOB) (22, 31). It is however possible that the low percentage of CCR5 expression in natural  
298 hosts is related indirectly to their resistance to disease. Indeed, while CCR5 is not a specific gut-  
299 homing receptor, it can induce migration to inflamed tissues (14). Such extremely low levels of  
300 CCR5<sup>+</sup> pDC in natural hosts could therefore be related to the lack of pDC accumulation in the gut  
301 after infection (32). Our results therefore suggest that evaluating the function of CCR5 in

302 seeding of viral reservoirs outside its role as a HIV co-receptor is warranted. Teasing out such  
303 mechanisms could be helpful for curative approaches.

#### 304 **Acknowledgments**

305 Funding: This work was supported by “Fondation AREVA”, the French National Agency for  
306 Research on AIDS and Viral Hepatitis (ANRS), Sidaction, “Fondation TOTAL” (to FBS), the French  
307 Ministry of higher Education and Research and Institut Pasteur. The funders had no role in study  
308 design, data collection and analysis, decision to publish, or preparation of the manuscript.

309 We are grateful to Christophe Joubert, Benoît Delache, Jean-Marie Héliès, Patrick Flament and  
310 the staff of the CEA animal facilities for outstanding work in animal care. We also sincerely thank  
311 the staff of the Institut Pasteur animal facility. We would like to thank Kathryn Faulkner for  
312 performing flow cytometric analyses on SM cells. We appreciate the excellent technical  
313 assistance of Claire Torres, Julie Morin, Aurélien Corneau and the TIPIV staff of the CEA. We  
314 would like to thank the Centre d’Immunologie Humaine (CIH) at Institut Pasteur for access to  
315 the FACSAria II cell sorter. We also would like to acknowledge the state-of-the-art National  
316 Center for Infectious Disease Models and Innovative Therapies (IDMIT). Viruses were kindly  
317 provided by A. David, D. Negre, F.-L. Cosset as well as J. Lifson and J. Bess, Jr. (AIDS & Cancer  
318 Virus Program, NCI at Frederick). SIVagm(gri-1) was obtained through the AIDS Research and  
319 Reference Program, Division of AIDS, NIAID, NIH, from J. Allan. We would like to thank A. Isaacs  
320 for reading of the manuscript and are grateful to J-P. Herbeuval and N. Smith for helpful  
321 discussion.

#### 322 **References**



- 323 1. **Sodora DL, Allan JS, Apetrei C, Brenchley JM, Douek DC, Else JG, Estes JD, Hahn BH,**  
324 **Hirsch VM, Kaur A, Kirchhoff F, Muller-Trutwin M, Pandrea I, Schmitz JE, Silvestri G.**  
325 2009. Toward an AIDS vaccine: lessons from natural simian immunodeficiency virus  
326 infections of African nonhuman primate hosts. *Nat Med* **15**:861-865.
- 327 2. **Diop OM, Ploquin MJ, Mortara L, Faye A, Jacquelin B, Kunkel D, Lebon P, Butor C,**  
328 **Hosmalin A, Barre-Sinoussi F, Muller-Trutwin MC.** 2008. Plasmacytoid dendritic cell  
329 dynamics and alpha interferon production during Simian immunodeficiency virus  
330 infection with a nonpathogenic outcome. *Journal of Virology* **82**:5145-5152.
- 331 3. **Beaumier CM, Harris LD, Goldstein S, Klatt NR, Whitted S, McGinty J, Apetrei C,**  
332 **Pandrea I, Hirsch VM, Brenchley JM.** 2009. CD4 downregulation by memory CD4+ T cells  
333 in vivo renders African green monkeys resistant to progressive SIVagm infection. *Nat*  
334 *Med* **15**:879-885.
- 335 4. **Paiardini M, Cervasi B, Reyes-Aviles E, Micci L, Ortiz AM, Chahroudi A, Vinton C,**  
336 **Gordon SN, Bosinger SE, Francella N, Hallberg PL, Cramer E, Schlub T, Chan ML, Riddick**  
337 **NE, Collman RG, Apetrei C, Pandrea I, Else J, Munch J, Kirchhoff F, Davenport MP,**  
338 **Brenchley JM, Silvestri G.** 2011. Low levels of SIV infection in sooty mangabey central  
339 memory CD4+ T cells are associated with limited CCR5 expression. *Nat Med* **17**:830.
- 340 5. **Pandrea I, Onanga R, Souquiere S, Mouinga-Ondeme A, Bourry O, Makuwa M, Rouquet**  
341 **P, Silvestri G, Simon F, Roques P, Apetrei C.** 2008. Paucity of CD4+ CCR5+ T cells may  
342 prevent transmission of simian immunodeficiency virus in natural nonhuman primate  
343 hosts by breast-feeding. *J Virol* **82**:5501-5509.
- 344 6. **Beignon AS, McKenna K, Skoberne M, Manches O, DaSilva I, Kavanagh DG, Larsson M,**  
345 **Gorelick RJ, Lifson JD, Bhardwaj N.** 2005. Endocytosis of HIV-1 activates plasmacytoid  
346 dendritic cells via Toll-like receptor-viral RNA interactions. *J Clin Invest* **115**:3265-3275.
- 347 7. **Jochems SP, Petitjean G, Kunkel D, Liovat AS, Ploquin MJ, Barre-Sinoussi F, Lebon P,**  
348 **Jacquelin B, Muller-Trutwin MC.** Modulation of Type I Interferon-Associated Viral  
349 Sensing during Acute Simian Immunodeficiency Virus Infection in African Green  
350 Monkeys. *J Virol* **89**:751-762.
- 351 8. **Donaghy H, Gazzard B, Gotch F, Patterson S.** 2003. Dysfunction and infection of freshly  
352 isolated blood myeloid and plasmacytoid dendritic cells in patients infected with HIV-1.  
353 *Blood* **101**:4505-4511.
- 354 9. **Brown KN, Wijewardana V, Liu X, Barratt-Boyes SM.** 2009. Rapid influx and death of  
355 plasmacytoid dendritic cells in lymph nodes mediate depletion in acute simian  
356 immunodeficiency virus infection. *Plos Pathogens* **5**:e1000413.
- 357 10. **Jacquelin B, Petitjean G, Kunkel D, Liovat AS, Jochems SP, Rogers KA, Ploquin MJ,**  
358 **Madec Y, Barre-Sinoussi F, Dereuddre-Bosquet N, Lebon P, Le Grand R, Villinger F,**  
359 **Muller-Trutwin M.** 2014. Innate Immune Responses and Rapid Control of Inflammation  
360 in African Green Monkeys Treated or Not with Interferon-Alpha during Primary SIVagm  
361 Infection. *PLoS Pathog* **10**:e1004241.
- 362 11. **Diop OM, Gueye A, Dias-Tavares M, Kornfeld C, Faye A, Ave P, Huerre M, Corbet S,**  
363 **Barre-Sinoussi F, Muller-Trutwin MC.** 2000. High levels of viral replication during  
364 primary simian immunodeficiency virus SIVagm infection are rapidly and strongly  
365 controlled in African green monkeys. *Journal of Virology* **74**:7538-7547.

- 366 12. **Jacquelin B, Mayau V, Targat B, Liovat AS, Kunkel D, Petitjean G, Dillies MA, Roques P,**  
367 **Butor C, Silvestri G, Giavedoni LD, Lebon P, Barre-Sinoussi F, Benecke A, Muller-**  
368 **Trutwin MC.** 2009. Nonpathogenic SIV infection of African green monkeys induces a  
369 strong but rapidly controlled type I IFN response. *J Clin Invest* **119**:3544-3555.
- 370 13. **Taaffe J, Chahroudi A, Engram J, Sumpter B, Meeker T, Ratcliffe S, Paiardini M, Else J,**  
371 **Silvestri G.** 2010. A five-year longitudinal analysis of sooty mangabeys naturally infected  
372 with simian immunodeficiency virus reveals a slow but progressive decline in CD4+ T-cell  
373 count whose magnitude is not predicted by viral load or immune activation. *J Virol*  
374 **84**:5476-5484.
- 375 14. **Meythaler M, Martinot A, Wang Z, Pryputniewicz S, Kasheta M, Ling B, Marx PA, O'Neil**  
376 **S, Kaur A.** 2009. Differential CD4+ T-lymphocyte apoptosis and bystander T-cell  
377 activation in rhesus macaques and sooty mangabeys during acute simian  
378 immunodeficiency virus infection. *J Virol* **83**:572-583.
- 379 15. **Gueye A, Diop OM, Ploquin MJ, Kornfeld C, Faye A, Cumont MC, Hurtrel B, Barre-**  
380 **Sinoussi F, Muller-Trutwin MC.** 2004. Viral load in tissues during the early and chronic  
381 phase of non-pathogenic SIVagm infection. *Journal of Medical Primatology* **33**:83-97.
- 382 16. **Muller MC, Saksena NK, Nerrienet E, Chappey C, Herve VM, Durand JP, Legal-**  
383 **Campodonico P, Lang MC, Digoutte JP, Georges AJ, et al.** 1993. Simian  
384 immunodeficiency viruses from central and western Africa: evidence for a new species-  
385 specific lentivirus in tantalus monkeys. *J Virol* **67**:1227-1235.
- 386 17. **Jin MJ, Hui H, Robertson DL, Muller MC, Barre-Sinoussi F, Hirsch VM, Allan JS, Shaw**  
387 **GM, Sharp PM, Hahn BH.** 1994. Mosaic genome structure of simian immunodeficiency  
388 virus from west African green monkeys. *EMBO J* **13**:2935-2947.
- 389 18. **Allan JS, Kanda P, Kennedy RC, Cobb EK, Anthony M, Eichberg JW.** 1990. Isolation and  
390 characterization of simian immunodeficiency viruses from two subspecies of African  
391 green monkeys. *AIDS Res Hum Retroviruses* **6**:275-285.
- 392 19. **Fomsgaard A, Hirsch VM, Allan JS, Johnson PR.** 1991. A highly divergent proviral DNA  
393 clone of SIV from a distinct species of African green monkey. *Virology* **182**:397-402.
- 394 20. **Aiken C.** 1997. Pseudotyping human immunodeficiency virus type 1 (HIV-1) by the  
395 glycoprotein of vesicular stomatitis virus targets HIV-1 entry to an endocytic pathway  
396 and suppresses both the requirement for Nef and the sensitivity to cyclosporin A. *J Virol*  
397 **71**:5871-5877.
- 398 21. **David A, Saez-Cirion A, Versmisse P, Malbec O, Iannascoli B, Herschke F, Lucas M,**  
399 **Barre-Sinoussi F, Mouscadet JF, Daeron M, Pancino G.** 2006. The engagement of  
400 activating FcγRs inhibits primate lentivirus replication in human macrophages. *J*  
401 *Immunol* **177**:6291-6300.
- 402 22. **Muller MC, Barre-Sinoussi F.** 2003. SIVagm: genetic and biological features associated  
403 with replication. *Front Biosci* **8**:d1170-1185.
- 404 23. **Lepelley A, Louis S, Sourisseau M, Law HK, Pothlichet J, Schilte C, Chaperot L, Plumas J,**  
405 **Randall RE, Si-Tahar M, Mammano F, Albert ML, Schwartz O.** 2011. Innate sensing of  
406 HIV-infected cells. *Plos Pathogens* **7**:e1001284.
- 407 24. **Kornfeld C, Ploquin MJ, Pandrea I, Faye A, Onanga R, Apetrei C, Poaty-Mavoungou V,**  
408 **Rouquet P, Estaquier J, Mortara L, Desoutter JF, Butor C, Le Grand R, Roques P, Simon**  
409 **F, Barre-Sinoussi F, Diop OM, Muller-Trutwin MC.** 2005. Antiinflammatory profiles

- 410 during primary SIV infection in African green monkeys are associated with protection  
 411 against AIDS. *J Clin Invest* **115**:1082-1091.
- 412 25. **Campillo-Gimenez L, Laforge M, Fay M, Brussel A, Cumont MC, Monceaux V, Diop O,**  
 413 **Levy Y, Hurtrel B, Zaunders J, Corbeil J, Elbim C, Estaquier J.** 2010. Nonpathogenesis of  
 414 simian immunodeficiency virus infection is associated with reduced inflammation and  
 415 recruitment of plasmacytoid dendritic cells to lymph nodes, not to lack of an interferon  
 416 type I response, during the acute phase. *Journal of Virology* **84**:1838-1846.
- 417 26. **Fomsgaard A, Muller-Trutwin MC, Diop O, Hansen J, Mathiot C, Corbet S, Barre-**  
 418 **Sinoussi F, Allan JS.** 1997. Relation between phylogeny of African green monkey CD4  
 419 genes and their respective simian immunodeficiency virus genes. *Journal of Medical*  
 420 *Primates* **26**:120-128.
- 421 27. **Zhou Y, Bao R, Haigwood NL, Persidsky Y, Ho WZ.** SIV infection of rhesus macaques of  
 422 Chinese origin: a suitable model for HIV infection in humans. *Retrovirology* **10**:89.
- 423 28. **Summerfield A, Auray G, Ricklin M.** Comparative dendritic cell biology of veterinary  
 424 mammals. *Annu Rev Anim Biosci* **3**:533-557.
- 425 29. **Ferrero I, Held W, Wilson A, Tacchini-Cottier F, Radtke F, MacDonald HR.** 2002. Mouse  
 426 CD11c(+) B220(+) Gr1(+) plasmacytoid dendritic cells develop independently of the T-cell  
 427 lineage. *Blood* **100**:2852-2857.
- 428 30. **Humes D, Emery S, Laws E, Overbaugh J.** 2012. A species-specific amino acid difference  
 429 in the macaque CD4 receptor restricts replication by global circulating HIV-1 variants  
 430 representing viruses from recent infection. *J Virol* **86**:12472-12483.
- 431 31. **Riddick NE, Hermann EA, Loftin LM, Elliott ST, Wey WC, Cervasi B, Taaffe J, Engram JC,**  
 432 **Li B, Else JG, Li Y, Hahn BH, Derdeyn CA, Sodora DL, Apetrei C, Paiardini M, Silvestri G,**  
 433 **Collman RG.** 2010. A novel CCR5 mutation common in sooty mangabeys reveals SIVsmm  
 434 infection of CCR5-null natural hosts and efficient alternative coreceptor use in vivo. *PLoS*  
 435 *Pathog* **6**:e1001064.
- 436 32. **Kwa S, Kannanganat S, Nigam P, Siddiqui M, Shetty RD, Armstrong W, Ansari A,**  
 437 **Bosinger SE, Silvestri G, Amara RR.** 2011. Plasmacytoid dendritic cells are recruited to  
 438 the colorectum and contribute to immune activation during pathogenic SIV infection in  
 439 rhesus macaques. *Blood* **118**:2763-2773.

440  
 441  
 442

443 **Figure 1. CD4 and CCR5 expression on blood plasmacytoid dendritic cells.** (A) CD4 and CCR5  
 444 expression on pDC (blue) and Lineage<sup>+</sup> cells (grey) of one representative Chinese cynomolgous  
 445 macaque, African green monkey, sooty mangabey and Indian rhesus macaque. (B) CD4  
 446 expression on pDC from SIV-negative Chinese rhesus macaques (n=8, open squares), Indian  
 447 rhesus macaques (n=1, open upward triangles), AGM (n=13, open circles) and SM (n=11, filled

448 grey circles). CD4 mean fluorescent intensity (MFI) on pDC was normalized (%) to the CD4 MFI  
449 on CD4<sup>+</sup> T cells. The horizontal, dashed line designates equal expression compared to CD4<sup>+</sup> T  
450 cells. (C) The percentage of CCR5<sup>+</sup> pDC was determined for SIV-negative Indian rhesus macaques  
451 (n = 11, open upward triangles), Chinese cynomolgous macaques (n = 2, open downward  
452 triangles), AGM (n = 7, open circles) and SM (n = 8, grey filled circles) and chronically SIV-  
453 infected Indian rhesus macaques (n = 8, open upward triangles), AGM (n=3, open circles) and  
454 SM (n = 8, grey filled circles). Symbols represent individual animals and lines and bars represent  
455 medians and interquartile ranges. \* Kruskal-Wallis, p < 0.05, \*\*\* Kruskal-Wallis, p < 0.001.

456 **Figure 2. Low CD4 expression on AGM pDCs.** (A) Dot plots showing the gating strategy used to  
457 identify pDCs, which are FSC/SSC, singlets, Lineage (CD3/CD20)<sup>-</sup> cells and HLA-DR<sup>+</sup> CD123<sup>hi</sup> cells,  
458 for one representative animal. (B) Low CD4 expression on AGM pDCs (n = 3) was confirmed  
459 using two additional monoclonal anti-CD4 antibodies (M-T466 and SFC112T4D11). Histograms of  
460 representative animals are shown, depicting CD4 expression on CD4<sup>-</sup> cells (grey, solid), pDCs  
461 (blue, solid with contour) and Lineage<sup>+</sup>CD4<sup>+</sup> cells (red, solid with contour). MFI values of CD4 for  
462 the three cell populations are shown in the table. (C) Intracellular and extracellular staining of  
463 AGM pDCs (n = 3). Histograms of a representative animal are shown, cell surface expression  
464 CD4 expression is depicted for CD4<sup>-</sup> cells (grey, solid) and for pDCs, intracellular (blue, solid with  
465 contour) and extracellular (green, solid with contour) expression is shown, indicating an absence  
466 of an intracellular CD4 pool in AGM pDCs. (D) Low CD4 expression was observed on pDCs from  
467 bone marrow (n = 1 AGM), LN (n = 1 AGM) and rectal biopsy (n = 1 AGM). Histograms depict  
468 CD4 expression on CD4<sup>-</sup> cells (grey, solid), pDCs (blue, solid with contour) and Lineage<sup>+</sup>CD4<sup>+</sup> cells  
469 (red, solid with contour). MFI values of CD4 are listed in the tables.

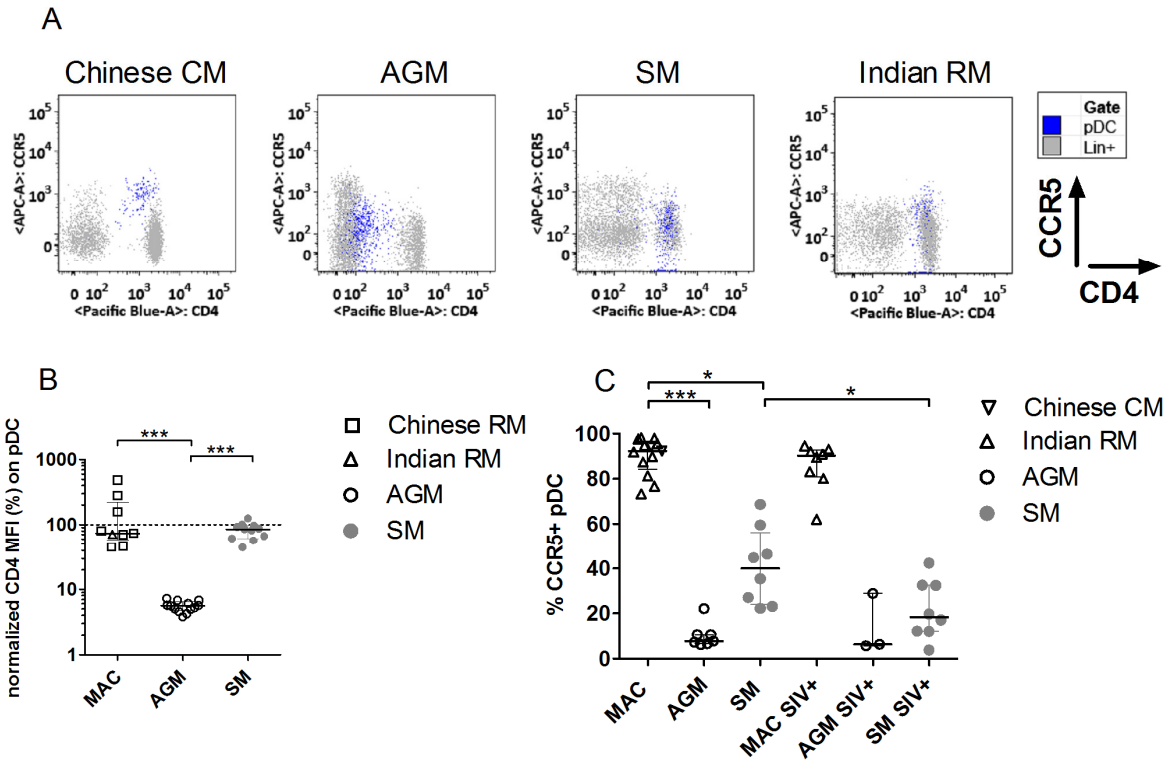
470 **Figure 3. SIV sensing capacity of AGM pDCs.** (A) SIVagm.sab92018 was used to stimulate AGM  
471 (n = 22) and SIVmac251 for Chinese rhesus MAC (n = 14) PBMCs. Alternatively, PBMCs were  
472 stimulated with HSV-1. (B) CD4 MFI was followed throughout SIVagm infection on four AGMs.  
473 Median and interquartile ranges are shown for CD4<sup>+</sup> Lineage<sup>+</sup> cells (red), pDCs (blue) and CD4<sup>-</sup>  
474 Lineage<sup>+</sup> cells (grey). (C) SIVagm-infected SupT1 cells and free virions were used to stimulate  
475 AGM PBMCs (n = 5). (D) SIVagm or AT2-inactivated SIVagm was used to stimulate AGM PBMCs  
476 (n = 8). Individual symbols represent distinct animals. Median and interquartile range are  
477 shown. Vertical dashes separate the different viral preparations used to test pDC sensing \*  
478 Friedman, p < 0.05.

479 **Figure 4. Viral and host determinants of SIV sensing by pDC.** PBMC from (A) AGM (n = 5-23)  
480 and (B) Chinese rhesus MAC (n = 2-15) were stimulated with medium (mock), five SIVagm, three  
481 SIVmac or HIV-1 (BAL) at three concentrations: 1500 ng/mL, 150 ng/mL and 15 ng/mL p24/p27.  
482 Median values are represented by a horizontal line (blue and red for SIVagm and HIV/SIVmac,  
483 respectively). \* Wilcoxon, p < 0.05, \*\* Wilcoxon, p < 0.01, compared to equal dose  
484 SIVagm.sab92018 stimulation. nd = not determined. Tox = cytotoxic in 18 hour culture. (C) AGM  
485 PBMC (n=10) were stimulated with medium (grey circle), 15, 150 or 1500 ng/mL p27 SIVmac251  
486 (red square) or SIVmac239 (blue triangle) for 18 hours after which viability was measured.  
487 Median and interquartile ranges are depicted. \* Wilcoxon, p < 0.05. (D) AGM PBMC were  
488 stimulated with HIV (n = 14), VSV-G pseudotyped HIV (n = 10), SIVmac251 (n = 10), VSV-G  
489 pseudotyped SIVmac251 (n=9) or SIVagm.sab92018 (n = 23) at 150 ng/mL p24 or p27. Median  
490 values and interquartile ranges are presented by a line and bars, respectively. \* Kruskal-Wallis,

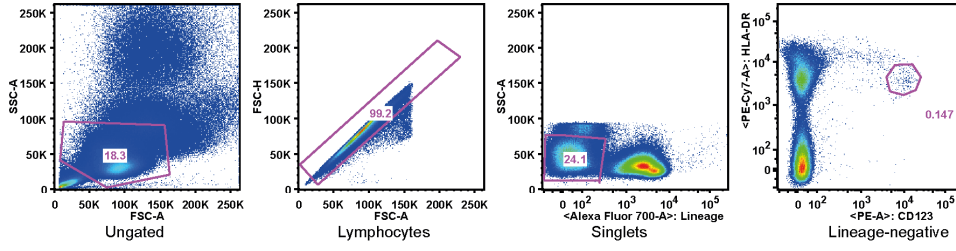
491  $p < 0.05$ , \*\* Kruskal-Wallis,  $p < 0.01$ , \*\*\* Kruskal-Wallis,  $p < 0.001$ . Symbols represent individual  
492 animals, horizontal dashed lines represent the limit of detection.

493 **Figure 5. In vivo pDC infection.** (A) PDC and CD4<sup>+</sup> T cells of chronically SIV-infected AGM (open  
494 circles,  $n = 7$ ) and Chinese rhesus MAC (black circles,  $n = 5$ ) were sorted from  $2 \times 10^8$  to  $4 \times 10^8$   
495 splenocytes, yielding a median of six thousand pDC after two subsequent sorts (purity 91%).  
496 CD4<sup>+</sup> T cells were also purified from lymph node (LN) cells (purity 97%). SIV DNA was normalized  
497 to CCR5 and represented as copies per million cells. Symbols represent individual animals. CD4<sup>+</sup>  
498 T cells in LN were infected to a higher extent in MAC than AGM (\* Mann-Whitney,  $p = 0.016$ ).  
499 SIV DNA copy numbers were similar between spleen and LN CD4<sup>+</sup> T in both species. (B)  
500 Fluorescence microscopy was performed on a LN of one chronically infected AGM. DAPI (blue)  
501 shows nuclei, CD123 (yellow) is expressed on pDC, SIV RNA (red) shows infected cells and NKp30  
502 (green) is a marker not expressed on pDC. The merge shows an overlap from CD123 and SIV  
503 signals.

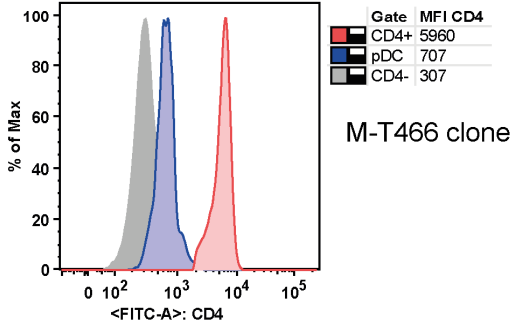
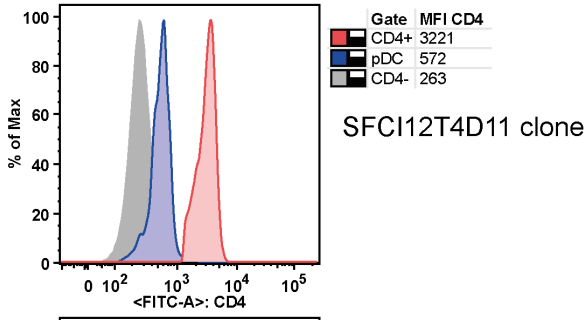
504 **Figure 6. CD4 and CCR5 expression on splenic AGM and MAC pDCs.** (A) CD4 expression was  
505 measured on pDCs from spleen of chronically SIV infected Chinese rhesus MACs ( $n=5$ ) and  
506 AGMs ( $n=5$ ). The mean fluorescent intensity (MFI) of CD4 on splenic pDCs was normalized (%) to  
507 the CD4 MFI on splenic CD4<sup>+</sup> T cells of the same animal. The horizontal, dashed line designates  
508 equal CD4 expression to CD4<sup>+</sup> Lineage<sup>+</sup> cells. Symbols represent individual animals and line and  
509 bars represent the median and interquartile range, respectively. (B) The percentage of CCR5<sup>+</sup>  
510 splenic pDCs was determined for SIV-infected Chinese rhesus MACs ( $n = 5$ ) and AGMs ( $n = 5$ ).  
511 Symbols represent individual animals and the line and bars represent the median and  
512 interquartile range. \*\* Mann-Whitney,  $p < 0.01$ .



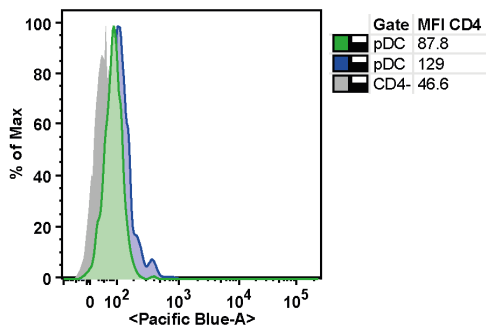
**A**



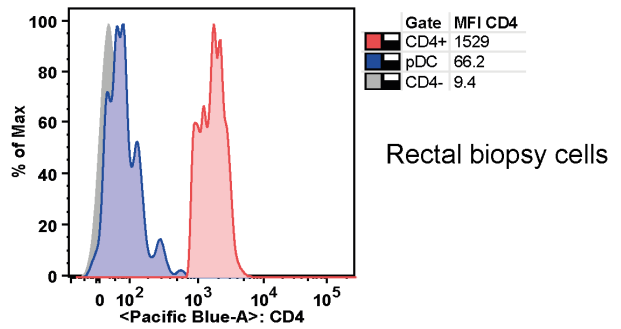
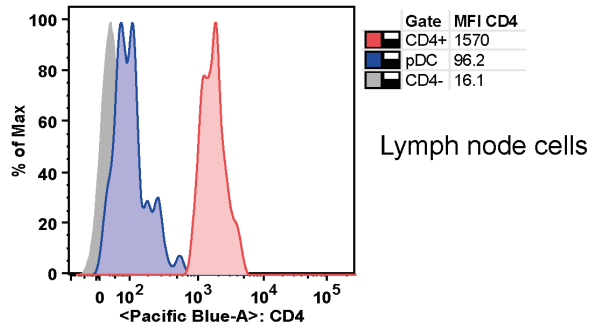
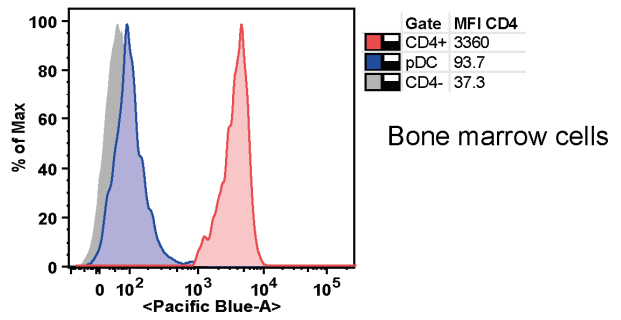
**B**



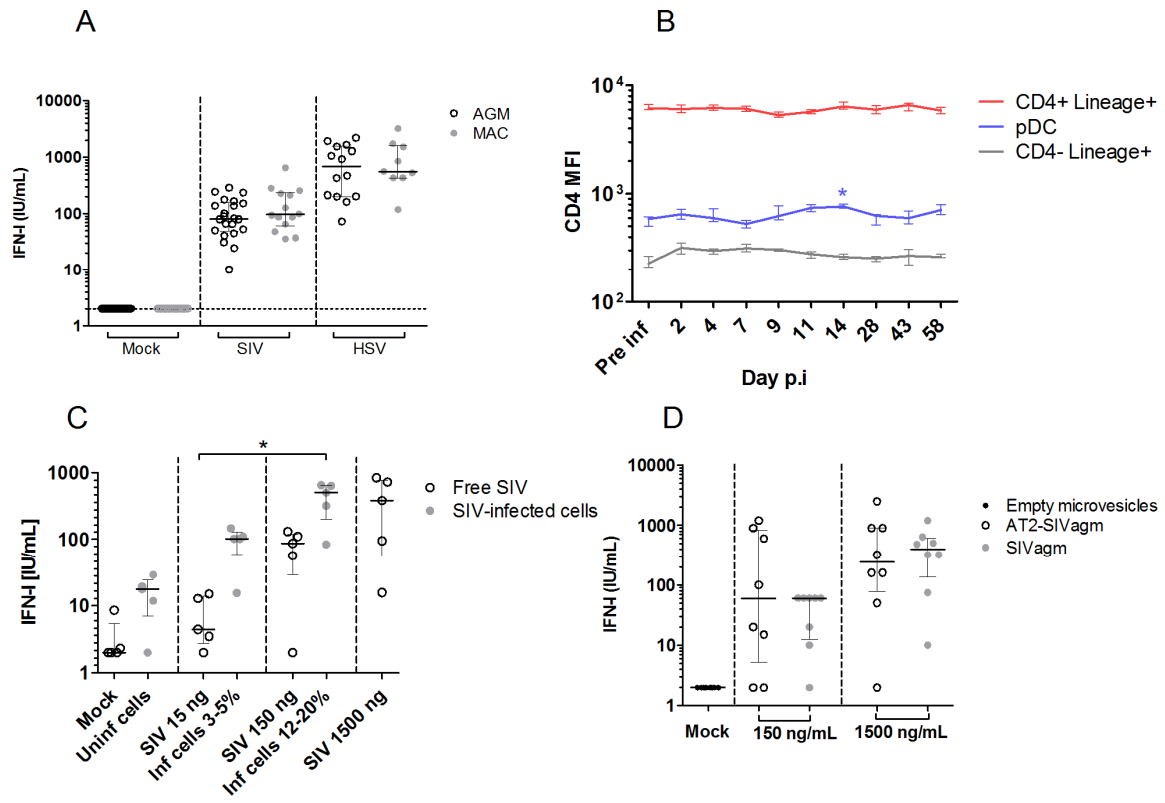
**C**

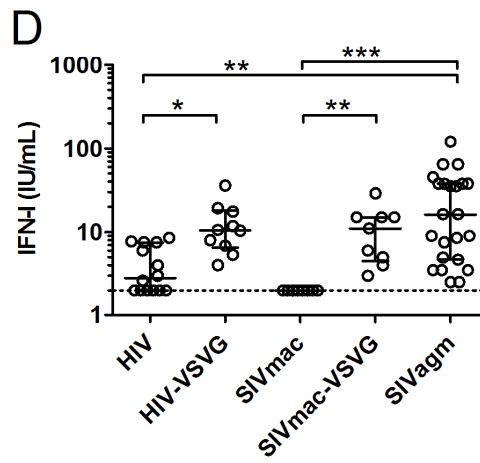
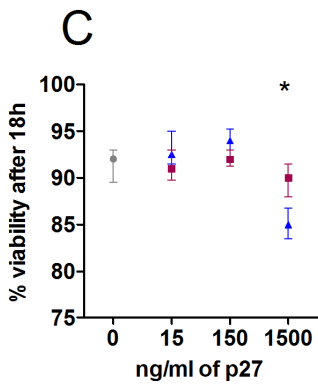
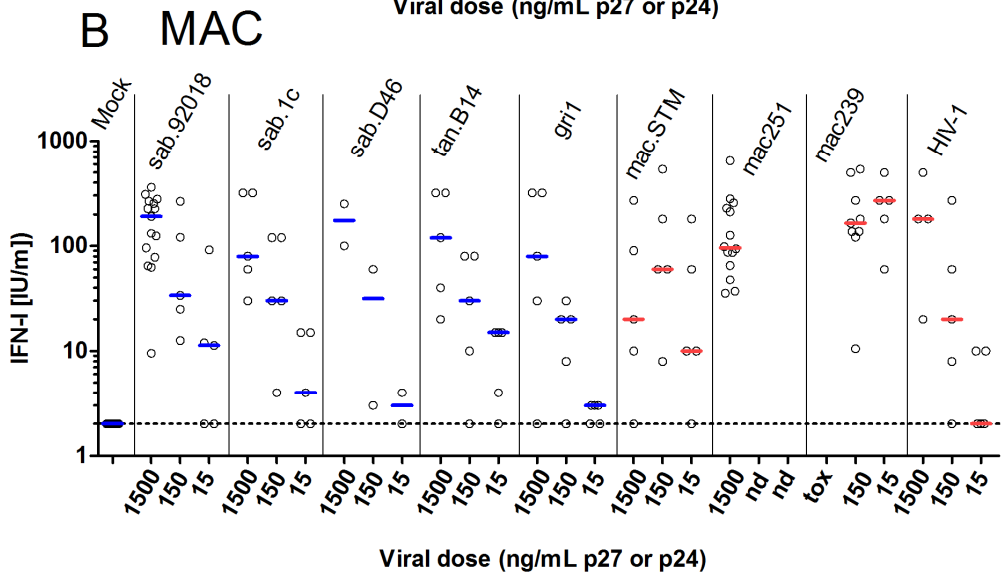
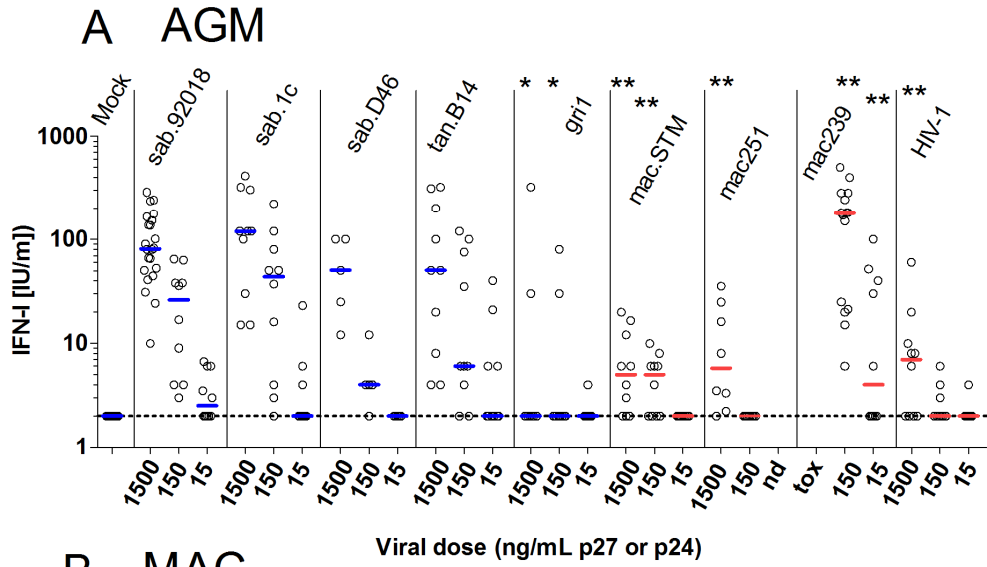


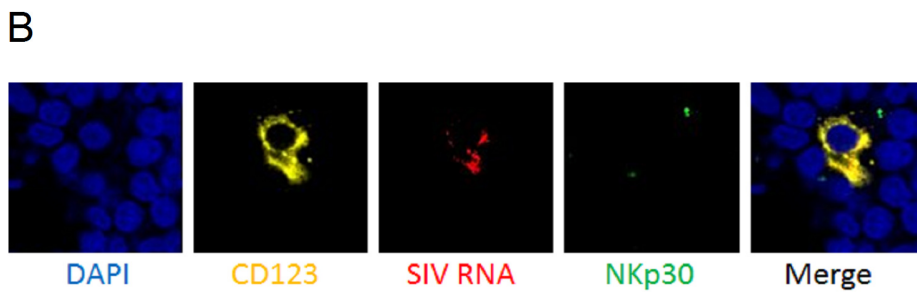
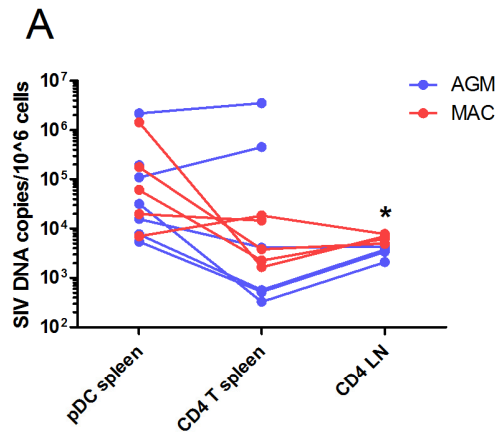
**D**



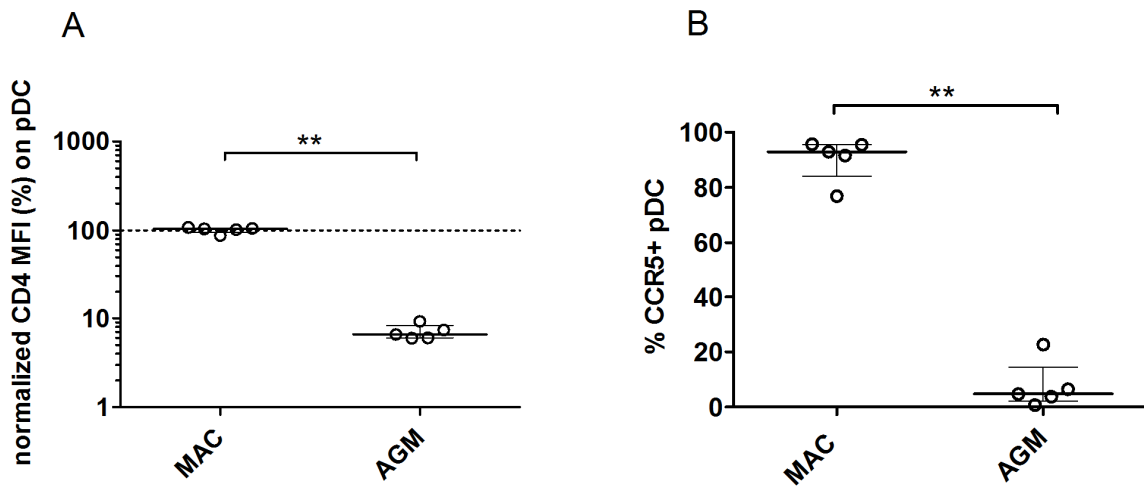








517



518